

Ever J. Barbero¹ and Ed Wen²

Coefficient of Thermal Expansion Compatibility Through Mechanical and Thermal Autofrettage in Metal Lined Composite Pipes

Reference: Barbero, E. J., and Wen, E. W., **Coefficient of Thermal Expansion Compatibility Through Mechanical and Thermal Autofrettage in Metal Lined Composite Pipes**, *ASTM STP 1436*, C. E. Bakis, Ed., American Society for Testing and Materials, West Conshohocken, PA, 2002.

Abstract

Coefficient of thermal expansion (CTE) compatibility between metal and composite is a major barrier for use of composites in applications that require a metal liner. The situation is critical for cryogenic applications because of the large temperature excursion to which the pipe is subjected. The paper demonstrates that CTE compatibility can be achieved through the use of autofrettage. Modeling techniques are introduced for the analysis of conventional mechanical autofrettage. Novel thermal autofrettage is proposed and demonstrated to be effective for those situations and material combinations for which conventional autofrettage is not feasible.

Keywords: autofrettage, cryogenic, composite, feed line, pipe, vessel.

Introduction

Metallic liners are used to eliminate gas permeation in composite pressure vessels and pipes. Typical applications include compressed natural gas (CNG) for automotive use, and storage and delivery of various substances for spacecraft applications. Most notable are the attempts to store and deliver cryogenic liquid hydrogen (LH2) and liquid oxygen (LOX) on experimental space delivery platforms such as X-33 and X-34 (Black 2000). All-composite feed lines for liquid Hydrogen (LH2) have been demonstrated (Tygielski 1997), but liquid oxygen (LOX) feed-lines have not. This is because composites typically are not able to pass the NASA STD 6001 compatibility test; especially, for high flow velocity feed lines with severe flow direction changes. Therefore, metallic lined pipes, although heavier than all-composite ones, are still of interest for spacecraft applications.

¹ Professor, Mechanical and Aerospace Engineering, West Virginia University, Morgantown, WV 26505-6106. ejbarbero@wvu.edu

² Manufacturing Engineer, Aurora Flight Sciences of West Virginia, 3000 East Benedum Industrial Drive, Bridgeport, WV 26330.

An alternative to autofrettage is to use thin metal liners along with permanent pressurization to prevent the liner from collapsing. For cryogenic applications, the large shrinkage of the metal caused by the cryogenic temperature can be controlled by pre-pressurization. This concept has been proposed for spacecraft pressure vessels (MacConichie 1984). It has not been used for feed lines because it increases the operational complexity, such as during emergency shutdown.

Although all-composite pressure vessels have been developed with polymeric liners to achieve low permeation rates, they have not penetrated the automotive market because low permeation rate has not been accepted by the consumers. The low strain to failure (or yield) of metals when compared to that of the PMCs dictates either use of a thick metal liner with a compliant fiber, such as Glass, or a stiff fiber such as Carbon fiber. The former option has had much more acceptance in the automotive market because of cost.

Another motivation for the use of metallic liners is the need to mitigate abrasion in high pressure pipes used for hydraulic fracturing by the oil industry (Briers 2001). While most of the oil industry uses thick walled metallic pipes, there is strong interest in reducing the weight of pipes in order to meet stringent OSHA regulations regarding handling weights.

The two challenges encountered in the design of hybrid metal-composite pressurized structures are: strain to failure (STF) compatibility and coefficient of thermal expansion (CTE) compatibility between the metal liner and the polymer matrix composite (PMC).

Autofrettage is a fabrication technique used to introduce pre-compression in a portion of a structure in order to extend the usable strain range of the material and to enhance fatigue life. It is used primarily for metallic thick-walled cylinders (mostly cannons) and for metal lined pressure vessels. The classical autofrettage techniques are to use interference fitting in cannons and pressurization in pressure vessels. Although interference fitting may use heating/cooling during assembly, it is a purely mechanical autofrettage because the material does not yield during the temperature excursion; in fact, the material remains elastic in most interference fittings. Pressurization is a mechanical autofrettage process that consists of applying enough pressure to exceed the yield strength of the metallic liner while the composite shell remains elastic. Upon de-pressurization, permanent deformations remain in the liner. As a result, the liner remains in compression and the composite shell remains in tension. Subsequent pressurization can span almost twice the strain range of the virgin metal since it is possible to autofrettage a liner up to its compression yield strength and then pressurize it up to its tensile yield strength.

Other types of autofrettage have been devised. Segall (1998) investigated localized autofrettage in order to enhance the fatigue life of thick-walled cylinders with cross-bores. Localized autofrettage of cannon tubes with evacuator holes was studied by Underwood (1996), who observed up to four-fold increase in fatigue life using 100% overstrain. Hussain (1980) also studied localized autofrettage on thick-walled tubes due to keyways, rifling, cracks, and so on. Low temperature autofrettage as proposed by Feng (1998) is essentially mechanical autofrettage but performed at low temperature because yield strength and modulus of the metal are higher at low temperature and the thermal strains accumulated during warm up to room temperature add to the autofrettage pre-

compression. Based on their finite element results, they concluded that autofrettage at low temperature was advantageous. Later we will introduce thermal autofrettage, which is completely different to autofrettage at low temperature.

Mechanical autofrettage, induced by pressurization, has been widely used in the CNG pressure vessel market (Lubin 1982, Liu and Hirano 1998) but not for pressurized pipe either cryogenic or not. The main difference between these applications is that pipes need a load transfer mechanism between the load bearing PMC and the metallic end fittings, as we show in this paper.

Coefficient of thermal expansion (CTE) mismatch exacerbates the problem of strain compatibility and it becomes critical for cryogenic applications where the temperature excursions could be as wide as 250⁰K (e.g., between liquid oxygen at 90⁰K to hot ambient at 340⁰K). We will show that mechanical autofrettage can be used to counteract the effect of CTE mismatch but with limitations stemming from the need to terminate the pipe in a metallic fitting. Limitations vary from metal to metal since CTE, modulus E, and yield strength σ_Y are interrelated in achieving the desired objective.

Mechanical Autofrettage

The idea of mechanical autofrettage is to pressurize the pipe to a proof pressure, which is higher than the operating pressure and lower than the burst pressure. Enough metal plasticity should be achieved during autofrettage so that the liner remains in compression upon unloading. The compression strain in the liner should not exceed the compression yield strain in order to avoid low cycle fatigue failure of the liner. In this work, the compression strain is limited to 95% of the yield strain (DOT-NGV2, 1995). The problem of cryogenic applications is that pre-compression changes upon cooling down to cryogenic operating temperature.

The desired amount of pre-compression can be achieved by varying metal thickness, composite thickness, fiber type, and laminate stacking sequence (LSS). Care must be taken to provide for enough composite strength as to meet the proof and burst pressure requirements.

Separate analysis techniques are developed here for two distinct sections of the pressurized pipe. The center section can be assumed to be uniform and absent of end effects. The end fittings require two- and three-dimensional analysis.

Center Section Autofrettage

We assume that the center section behaves as an infinitely long cylinder under radial pressure and free of end effects. The liner is elastic-perfectly plastic with no Bauschinger effect. We use the maximum strain criterion for the composite and the maximum stress criterion for the liner. We assume sliding contact between liner and composite to simulate a fully debonded interface. When the diameter-to-thickness ratio is larger than 20, the hoop and longitudinal stress are

$$N_H = t\sigma_H = p r \quad , \quad N_L = t\sigma_L = p r/2 \quad (1.1)$$

where p , r , t are the internal pressure, inner radius, and pipe thickness respectively. We use stress resultants in the hoop and longitudinal directions N_H , N_L , because of the inhomogeneity of the material. In that sense, the hoop and longitudinal stresses in (1.1) should be thought of as average stress values and not point stress values

anywhere through the thickness of the pipe wall. Force equilibrium between the internal pressure and the hoop loads yields

$$\sigma_m t_m + \sigma_c t_c = p r \quad (1.2)$$

where the subscripts m , c , indicate metal and composite respectively. Again, the stress in the composite is an average value not to be confused with any point stress value anywhere through the thickness of the composite wall.

We illustrate mechanical autofrettage in Fig. 1. The vertical axis corresponds to hoop stress, either liner or composite, while the horizontal axis corresponds to liner and composite strains, which are identical due to strain compatibility. We accomplish mechanical autofrettage by pressurizing the pipe at constant temperature, usually at room temperature. Starting at point 0, both metal and composite sustain tensile stress proportional to the applied pressure. The liner yields at point Y and sustains plastic strain until point 1m. Partial pressure release unloads the liner to point A, where it sustains no stress but has permanent strain

$$\varepsilon_0 = \varepsilon_{1m} - E_m \sigma_Y \quad (1.3)$$

Note that this strain is computed with no thermal expansion and thus corresponds to autofrettage performed entirely at constant temperature, usually at room temperature. Total pressure release puts compression stress on the liner at point 3m. At this point, the hoop stress becomes

$$\sigma_m = E_m (\varepsilon_m - \varepsilon_0) \quad (1.4)$$

where ε_0 is the metal strain when the metal stress is zero, at autofrettage temperature, indicated by point A in Fig. 1. Note that this is not an un-pressurized state since the composite is in tension. At this point, the equilibrium strain in both liner and composite is obtained from (1.2) and (1.4) as

$$\varepsilon = \varepsilon_m = \varepsilon_c = \frac{t_m E_m \varepsilon_0}{t_c E_c + t_m E_m} \quad (1.5)$$

Using the equations developed so far, we analyze the center section of the pipe for six load situations.

The first is at autofrettage load, denoted as point 1c and 1m in the composite and metal respectively. The proof and autofrettage pressure do not need to coincide. In CNG vessel production, they are set at the same value, so that the actual proof testing becomes the autofrettage process, thus eliminating the additional cost of separate autofrettage. In this work we do not impose such restriction because it leads to a sub-optimal design. We rather choose the value of autofrettage pressure that results in maximum allowable pre-compression at zero pressure, hot temperature ambient (HTA, 340⁰K), which in this study is set at 95% the compressive yield strain of the liner. If the code of practice mandates a fixed value of proof pressure, such as 150% operating pressure, then the autofrettage pressure need to be at least that high.

The second point is burst pressure, denoted by point 2c and 2m in Fig. 1. Autofrettage has no effect on the burst pressure capability of the pipe, as it is controlled by the composite. The liner contribution to force equilibrium (1.2) is capped by yield strength of the metal. The thickness of the composite should be sufficient to provide adequate burst pressure capability, which is normally mandated by the applicable code of practice (Tygielski 1997). One pipe out of each production lot will be tested to failure to

demonstrate burst capability. It must be noted that the burst pressure requirement provides a minimum thickness limit for the design of the composite shell.

The third point is zero pressure RTA, represented by 3c and 3m in Fig. 1. Equation (1.5) gives the strain in both composite and liner at RTA. Subsequently, the pipe may experience hot and cold un-pressurized conditions. The hot condition is typical of launch pad conditions. We took 340⁰K in our example. The stress-strain state moves to 4c/4m in the diagram. The metal expands from 3m to 4m. The composite stress-strain state moves along a line from 3c to 4c to maintain strain compatibility. The temperature effect only, without autofrettage, is described by (Barbero 1999, sect. 6.6)

$$\varepsilon = \frac{t_m E_m \alpha_m \Delta T}{t_c E_c + t_m E_m} \quad (1.6)$$

$$\sigma_m = E_m (\varepsilon - \alpha_m \Delta T) \quad (1.7)$$

Then, using superposition, the dashed line 3m-4m-5m in Fig. 1 is the result of changes in temperature as

$$\varepsilon = \frac{t_m E_m (\varepsilon_0 + \alpha_m \Delta T)}{t_c E_c + t_m E_m} \quad (1.8)$$

$$\sigma_m = E_m (\varepsilon - \varepsilon_0 - \alpha_m \Delta T) \quad (1.9)$$

The compressive stress resulting from autofrettage plus thermal expansion at hot condition becomes the liner sizing criteria, thus mandating the minimum thickness. This becomes the crucial constraint with regards to weight because of the higher density of the metal liner has a major impact on overall weight. We kept the maximum pre-compression strain in the liner including hot thermal expansion under 95% of the yield strain.

The cold condition represents an un-pressurized pipe filled with the cryogenic fluid. This is typical of engine chill-down for liquid fuel rocket propulsion systems. We took cryogenic LOX temperature at 90⁰K. The composite unloads from 3c to 5c as the metal contracts from 3m to 5m. This introduces another restriction on the design at point 5m. The pre-compression strain needs to be kept negative (compression) so that liner-composite contact pressure remains positive. This is to prevent any possibility of liner debonding. In our example, we kept the minimum pre-compression in the liner to 5% of the yield strain.

Center Section Flight Loads

Analysis of operation at cryogenic temperature should take into account the improvements in liner modulus and tensile yield strength at low temperature. As a result, the line 5m-6m-7m has a higher slope and higher yield value that at RTA. Our example is based on estimated operating loads that include internal pressure, cryogenic operation, as well as flight loads. The structural analysis group commonly supplies these, and they take into account acceleration, vibrations, and other effects.

The flight loads consists of internal pressure and a set of beam loads at the two ends of each pipe section. The beam loads are: two bending moments, two shear forces, one torque, and one axial force. We use these values to compute the stress resultants $N = \{N_x, N_y, N_{xy}\}$ on the hybrid laminate (liner plus composite). Assuming that the pipe is a thin walled beam, the flight loads yield only inplane stress resultants, with $M = \{M_x, M_y,$

$M_{xy} = \{0\}$. Of all the flight conditions, we select that which yields the highest values for the stress resultants.

We use the inplane stress resultants and the laminate stiffness matrix to compute the midplane strains and curvatures using classical lamination theory as follows

$$\begin{Bmatrix} \varepsilon \\ \kappa \end{Bmatrix} = \begin{bmatrix} \alpha & \beta \\ \beta & \delta \end{bmatrix} \left(\begin{Bmatrix} N \\ M \end{Bmatrix} + \begin{Bmatrix} N_T \\ M_T \end{Bmatrix} \right) \quad (1.10)$$

where

$$\begin{bmatrix} \alpha & \beta \\ \beta & \delta \end{bmatrix} = \begin{bmatrix} A & B \\ B & D \end{bmatrix}^{-1}$$

where A, B, D , are the extension, coupling, and bending 3x3 stiffness matrices of the laminate (Barbero 1999); ε, κ , contain the three components of the midplane strain and curvature, respectively; N, N_T , are the inplane mechanical and thermal stress resultants, respectively; and $M = M_T = \{0\}$.

Since the laminate is not symmetric due to the liner on the inside of the pipe, we get nonzero curvatures. But the axisymmetric, prismatic geometry of the pipe, effectively prevents these curvatures from taking place. In other words, the pipe wall is constrained to remain essentially circular and the pipe to remain essentially straight. That means that there exist a set of internal moments $M = \{M_x, M_y, M_{xy}\}$ to enforce zero curvature $\kappa = \{0\}$. Setting $\kappa = \{0\}$ in (1.10) we get the matrix equation

$$M = -\gamma^{-1} \beta N \quad (1.11)$$

from which we find the magnitude of the internal moments. Finally, we plug the midplane loads N and the internal moments M into (1.10) to find the midplane strains ε generated by flight loads. We use these to evaluate the safety factor according to maximum strain criterion in the composite and maximum stress criterion in the liner.

The pipe flight loads condition is denoted by point 6c-6m in the diagram. The liner must remain in the elastic range with a safety factor to avoid low cycle fatigue under operating conditions.

The burst pressure at cryogenic temperature may be slightly lower or higher than burst at RTA because the starting loading point is point 5c, not 0, and because the metal yield strength is higher at low temperature. That is, the composite has autofrettage/cryogenic induced tensile pre-stress at zero internal pressure and cryogenic temperature (point 5c). Such pre-stress limits the pressure excursion up to point 7c.

For comparison we used eight different liner metals with properties given by Wen (2001). In Table 1, we present the safety factor for eight liner metals, as well as the percentage weight savings using an all-aluminum pipe as baseline. We did not account for the weight of the end fittings since the analysis in this section is for an infinitely long pipe. The composite was $[0/90]_S$ IM7-977-6 (Wen 2001).

We checked the accuracy of the approximate solution (1.1)-(1.11) by finite element modeling of the center section (Table 2). We generated the mesh using IDEAS and we solved it in ABAQUS because it allows temperature dependent material properties. We used axisymmetric elements and contact elements between the liner and composite. Since neither ABAQUS nor IDEAS have laminated axisymmetric elements, and a full 3D model including elastoplasticity would be too expensive, we calculated equivalent orthotropic properties using lamination theory (Barbero 1999) and entered

them as orthotropic properties for the axisymmetric elements. We had to take great care to express the equivalent properties in the correct element coordinate system. We performed a convergence study to assess convergence of the numerical solution as a function of the number of elements through the thickness of the liner and the element aspect ratio. Since the center section is in a state of generalized plane strain, even one element through the thickness and an aspect ratio of four throughout the whole mesh gave results within 10% of the approximate solution.

Center Section Buckling

Compressive stress in the liner due to either mechanical or thermal autofrettage may cause the liner to buckle under the external pressure exerted by the composite shell. The buckling mode is that of a thin liner constrained by a comparatively rigid composite outer shell. Therefore, the buckling mode must include membrane deformation and all the buckling deformations must occur to the interior of the pipe. An approximate value for the critical pressure p_{CR} for this type of buckling was proposed by Glock (1977)

$$p_{CR} = 0.969 \left(\frac{AR^2}{I} \right)^{2/5} \left(\frac{E_m I}{R^3} \right) \quad (1.12)$$

where E_m is the modulus of the liner, R is the inner radius of the pipe, A and I , are the area and moment of inertia of a unit width of the liner wall. The solution is set up in this way to account for rib stiffened liner walls. The predicted critical pressure is lower than the actual contact pressure computed by using (1.5) and

$$p = \frac{t_m E_m \varepsilon}{R} \quad (1.13)$$

Therefore, an adhesive must be used to provide for liner stability at the cold un-pressurized condition. This is always the case when the liner is very thin. Two methods have been used commercially for thin liner pressure vessels. One method is permanent pressurization. The other method is to use an adhesive to prevent buckling. In this case the adhesive is not highly loaded but it acts as bracing against buckling. Therefore, a small amount of bond strength is sufficient to prevent buckling when it is applied uniformly over the entire liner-composite interface. Dexter Hysol EA9696 was used by Carleton PTD (2001) to prevent buckling of non-cryogenic tank.

End Fittings Autofrettage

The main difference between classical applications, such as pressure vessels and cannons, and feed line pipes, is the need for end fittings. End fittings create a sudden change of stiffness that complicates the autofrettage process. We used a simple design of the flange and transition section to develop the analysis methodology and to demonstrate feasibility. Undoubtedly, much weight savings could be realized by optimizing this section. Flange joints commonly join rocket engine feed-lines and deflections control their design in order to prevent leaks. Since the stiffness of our composite laminate was similar to that of aluminum, we made our flanges of the same thickness as the current aluminum design. We used 0.75" thick flange with a 0.5" inner radius to connect the flange with the pipe. All plies continue through the radius without termination, which is

overly conservative and could be improved (Harvey and Kremer 1997). We kept a 16:1 ply drop-off ratio to taper down the flange thickness into the pipe center section.

The flange section is so thick and stiff that it does not allow mechanical autofrettage. In other words, internal pressure alone cannot expand the pipe enough to produce plastic strains in the liner. Under a full temperature excursion from RTA down to cryogenic temperature, the liner to composite adhesive would have to keep the metal from shrinking away from the rigid composite flange. This is not a desirable situation because it would require qualification of adhesive bond, which is a very difficult process. Even if the adhesive could hold the liner, some metals with high CTE may yield in tension under thermal load alone. Assuming a rigid composite flange perfectly bonded to the liner, we estimate the full thermal strain from a temperature drop from RTA to cryogenic operating temperature to be

$$\sigma = \frac{E_m \alpha_m \Delta T}{1 - \nu_m} \quad (1.14)$$

where the Poisson's ratio is included to account for biaxial thermal shrinkage. For an acceptable design, this thermal stress would have to be under 95% of the tensile yield of the metal, or equivalently have a safety factor above 1.05. We can see in Table 2 that Aluminum 2219 and Nickel do not satisfy this condition because of their high CTE values. On the other hand, Nickel Alloy 8020 and Inconel 718 do not yield under thermal load alone because of their lower CTE. In any case, holding the thermal loading with an adhesive is questionable, which motivated us to propose thermal autofrettage, described later in this paper.

Transition Section

We kept a 16:1 ply drop-off ratio to taper down the flange thickness into the pipe center section. The 16:1 ratio is overly conservative and refining the design here could save a lot of weight.

We made an axisymmetric finite element model of the flange and transition regions. Between the liner and composite, we included film adhesive EA 9696 (Wen 2001) with thickness 0.010" for which it delivers its maximum flat wise tensile strength. In practice, a flange joint is in contact with a mating flange and held in place by a backup ring. Bolts run through the backup ring and both mating flanges to join the assembly. In an axisymmetric model we cannot model individual bolts, so we modeled the effect of the mating flange and backup rings by contact elements. This is a reasonable model since very close bolt spacing and very rigid backup rings are common in practice to avoid leaks.

Internal pressure is effective to produce autofrettage up to the beginning of the ply drop off region (Fig. 2). The transition to no autofrettage is gradual for all materials due to the gradual increase in stiffness of the composite in the transition area. The FEM results confirm that the flange and transition area do not experience autofrettage from internal pressure. Furthermore, the FEM results confirmed our prediction (1.14); that is, cryogenic loading yields Aluminum 2219 and Nickel liners but not Nickel Alloy 8020 or Inconel 718 (Table 2).

Thermal Autofrettage

The composite shell in the flange and transition regions are too stiff to allow for mechanical autofrettage. A temperature drop to cryogenic operation temperature would cause the liner to pull away from the composite. Furthermore, the thermal strain would cause yield of Aluminum and Nickel as indicated in Table 2. Therefore, we propose to use thermally induced yield to induce thermal autofrettage. That is, we propose to cool the pipe to a temperature lower than the operating temperature so that the thermally induced plastic deformation sets the liner in compression at RTA in a similar fashion as what we can accomplish with mechanical autofrettage. Cooling media available include liquid nitrogen (LN₂) at 77⁰K and liquid Helium (LHe) at 4⁰K. A mixture of LHe and LN₂ can be used to achieve any temperature in between.

Table 2 shows that the flange area of Aluminum and Nickel yield under thermal strain. Introducing thermal autofrettage in LN₂ makes those same two metals, achieve acceptable safety factors as indicated in Table 3 for 90⁰K.

With thermal autofrettage, care must be taken that the metal does not yield in tension at the hot condition. This is because the amplitude of the elastic strain excursion is always twice the yield strain of the metal. With thermal autofrettage, the elastic strain excursion starts at the autofrettage temperature. As the material gets hot, it expands, thus using up some of its strain capability. Table 3 contains the safety factors at the hot condition of 340⁰K. We can see that aluminum and nickel almost satisfy the desired 1.05 safety factor. That is, the metals are at 95% of their tensile yield when hot. Since liner yield is not an ultimate failure event, a safety factor close to 1.05 is acceptable (DOT-NGV2, 1995).

Conclusions

The approximate model of mechanical autofrettage is shown to be accurate for the analysis of metal composite lined tubes subject to large temperature excursions. The model is applicable to material selection, specifically metal selection, to satisfy CTE compatibility requirements with the composite shell. A novel thermal autofrettage method is proposed for those situations for which pressurization alone cannot produce the required autofrettage pre-compression. It is shown that even those metals with largest CTE values can be used as liners by introducing thermal autofrettage. Analysis techniques are presented to check the design at every stage of the fabrication, autofrettage, and operation of cryogenic feed lines.

Acknowledgements

Partial support for this research was provided by NASA Space Grant Consortium Faculty Initiation Grant and by Halliburton Energy Systems, which is appreciated.

References

Barbero, E. J., 1999, "Introduction to Composite Materials Design," Taylor & Francis, Philadelphia, 321-327.

Black, S., 2000, "X-34 composite liquid oxygen tank a first," High Performance Composites, Vol 8, No 4, 52-54.

Briers, W., 2001, "The design and analysis of a hybrid steel/composite pipe for high pressure application," MS Thesis, West Virginia University, Mechanical Aerospace Engineering Department.

DOT-NGV2, 1995, Code of Federal Regulations, Federal Register, Washington, DC.

Feng, H., Mughrabi, H. and Donth, B., "Finite-Element Modelling of Low-Temperature Autofrettage of Thick-Walled Tubes of the Austenitic Stainless Steel AISI 304 L: Part I. Smooth Thick-walled Tubes," Modelling and Simulation in materials Science and Engineering 6, 1998, p. 51-69.

Glock, D., 1977, "Überkritisches Verhalten eines starr ummantelten Kreisrohres bei Wasserdruck von außen und Temperaturdehnung," Der Stahlbau, Vol 7, 212-217. ("The over-critical behavior of a rigidly encased pipe under outer-hydrostatic pressure and thermo-stretch," translated by Li, Shi.)

Harvey, W.A., Kremer, J.S., 1997, "Design, process development, and fabrication of an all IM7/977-2 12 inch diameter pressurized fuel line required to operate at -423F while bolted to an aluminum valve," 42nd International SAMPE Symposium, 839-853.

Hussain, M. A., Pu, S. L., Vasilakis, J. D. and O'Hara, P., "Simulation of Partial Autofrettage by Thermal Loads," Journal of pressure Vessel Technology Technical Briefs, August 1980, Vol. 102, p. 314-318.

Liu, J. and Hirano, T., "Design and Analysis of FRP Pressure Vessels with Load-Carrying Metallic Liners," PVP-Vol. 368, Analysis and Design of Composite, Process, and Power Piping and Vessels, 1998, p. 95-101.

Liu, J. and Hirano, T., 1998, Design and Analysis of FRP Pressure Vessels with Load-Carrying Metallic Liners, PVP-Vol. 368, Analysis and Design of Composite, Proces, and Power Piping Vessels, 95-101.

Lubin, G. et al, Handbook of Composites, Van Nostrand Reinhold Company, 1982.

MacConochie, I., et.al., 1984, "Reusable cryogenic-liquid tank with replaceable liner," NASA Tech Brief LAR-14172.

Segall, A. E., Tricou, C., Evanko, M. and Conway, Jr., J. C., "Localized Autofrettage as a Design Tool for the Fatigue Improvement of Cross-Bored Cylinders," Journal of Pressure Vessel Technology, Vol. 120, November 1998, p. 393-397.

Tygielski, P., 1997, "Development of a Composite Feedline for the Clipper Graham Vehicle," 33rd AIAA/ASME/SAE/ASEE Joint Propulsion Conference & Exhibit, AIAA 97-2673.

Underwood, J. H., Parker, A. P., Corrigan, D. J. and Audino, M.J., "Fatigue Life Measurements and Analysis for Overstrained Tubes with Evacuator Holes," Transactions of the ASME, Vol. 118, November 1996, p. 424-428.

Wen, E. (2001) PhD Dissertation Defense, West Virginia University, Morgantown, WV 26505-6106.

Table 1. Safety factors at various points of the autofrettage and operating conditions

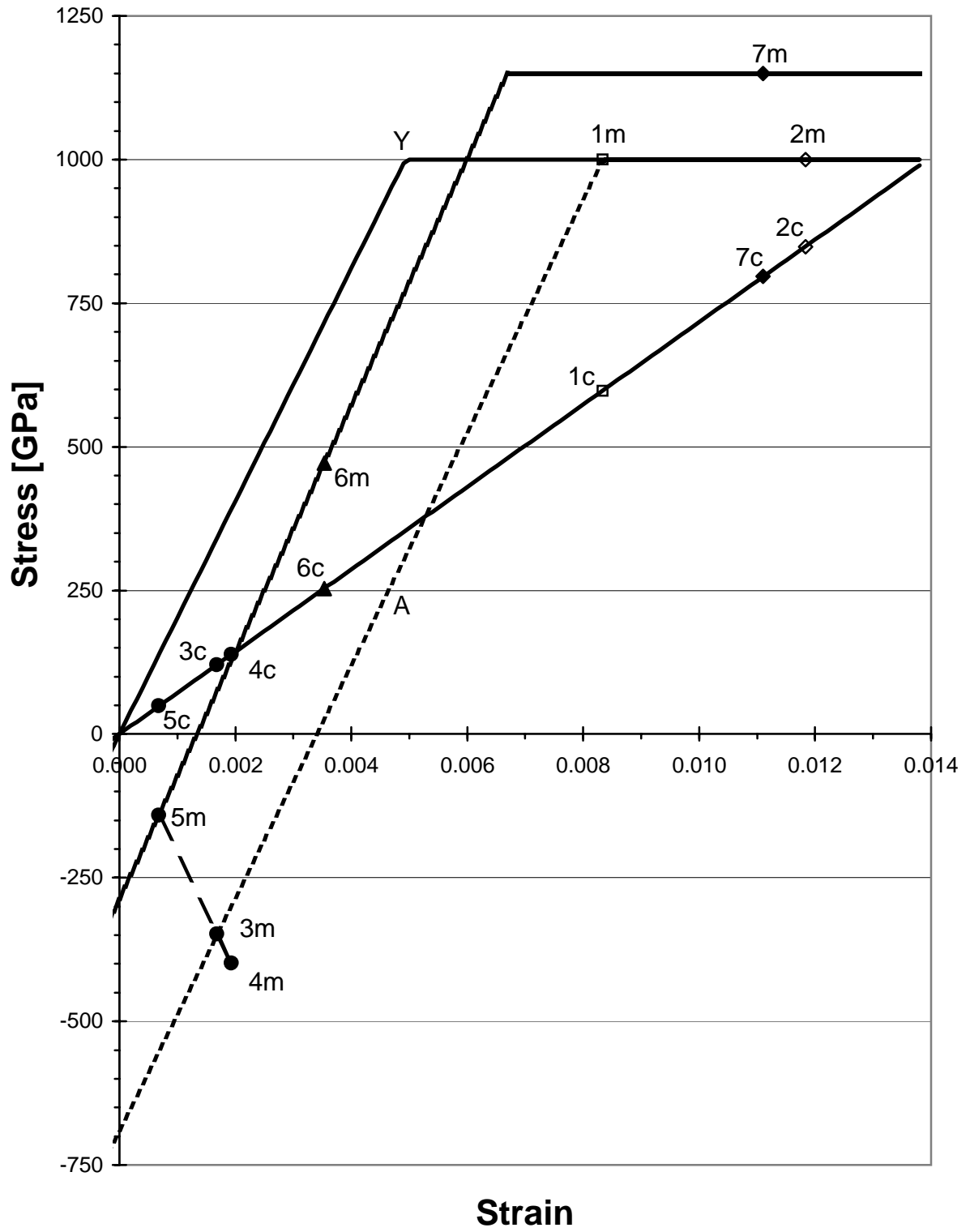
	Diagram Reference Point	Liner					All metal
		Inconel	Aluminum 2219	Nickel	Nickel Alloy	Invar 36	Aluminum 2219
Composite thickness (mm)		0.7315	0.7315	0.7315	0.7315	2.9210	0.0
Liner thickness (mm)		0.254	0.635	0.254	0.254	0.254	1.8034
CTE @ 90 ⁰ K		9.9	18	19.188	7.128	2.7	18
Proof Factor @ 298 ⁰ K	#1	2.0	1.7	1.8	1.5	1.8	1.2
Burst Factor @ 298 ⁰ K	#2	2.8	2.5	2.5	2.5	8.5	1.9
Burst Factor @ 90 ⁰ K	#7	2.9	2.6	2.6	2.6	8.6	2.3
Metal SF @ 298 ⁰ K un-pressurized	#3m	3.1	1.4	1.3	2.1	1.6	-
Metal SF @ 339 ⁰ K un-pressurized	#4m	2.6	1.2	1.08	1.8	1.5	-
Metal SF with Flight Loads @ 90 ⁰ K	#6m	2.1	1.4	1.5	1.6	2.7	1.8
% weight savings		40	45	36	36	-18	0

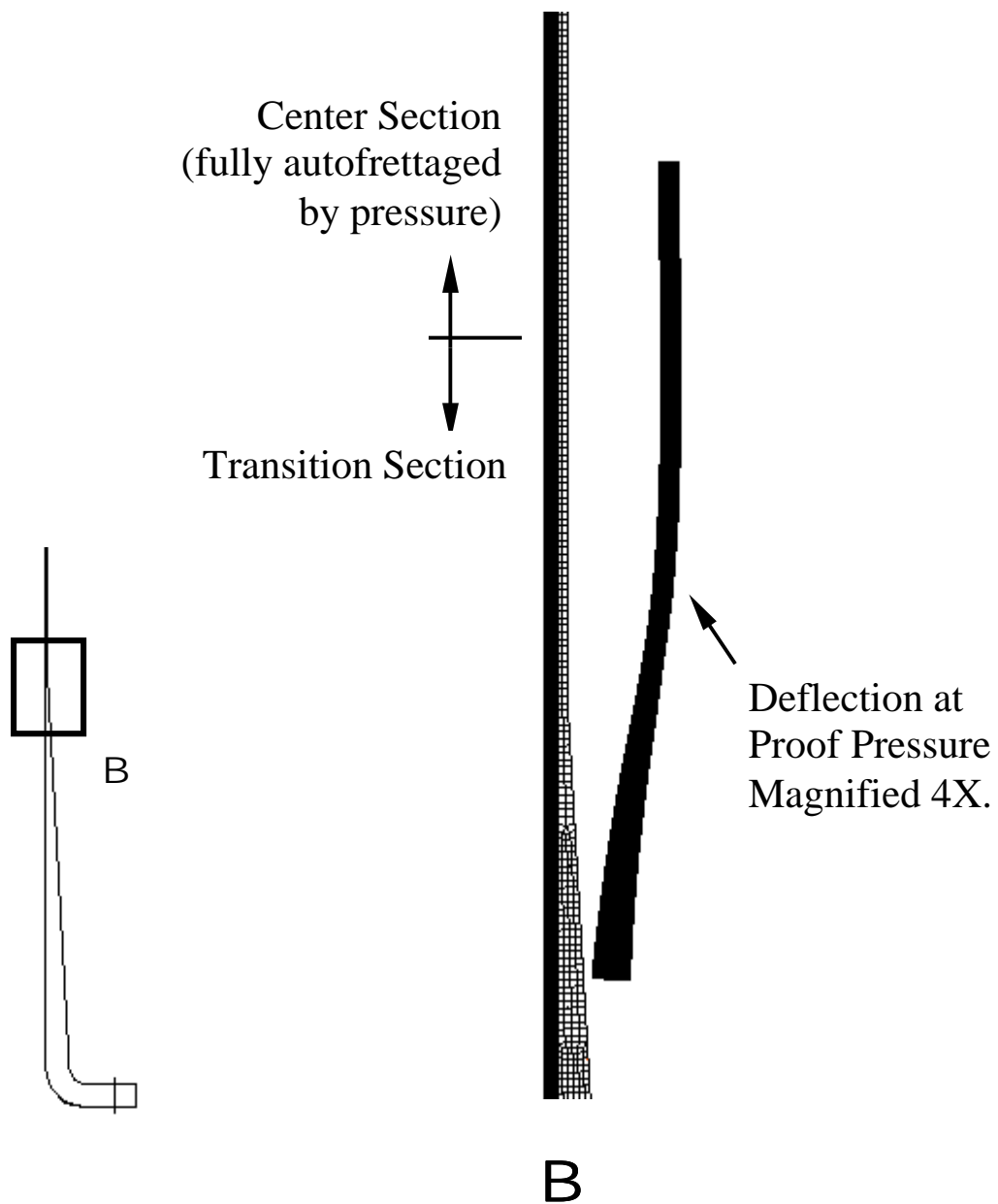
Table 2. Safety factors for liner tensile yield at cryogenic temperature (-298F) and zero pressure in the flange region.

Liner Material	1D model	FEM
Al 2219	0.64	0.67
Nickel	0.71	0.75
Nickel Alloy	1.90	1.92
Inconel	1.84	1.87

Table 3. Safety factors for liner yield at cryogenic temperature (-298F) and zero pressure in the flange region with thermal autofrettage.

Liner Material	90 ⁰ K un-pressurized liner tensile yield	340 ⁰ K un-pressurized liner compressive yield
Al 2219	1.03	1.04
Nickel	1.05	1.15





Barbero, E. J. and Wen, E.A. , Figure 2